

## VAT PHOTOPOLYMERIZATION ASSISTED ADDITIVE MANUFACTURING OF TITANIUM SCAFFOLDS

<sup>1</sup>Lenka DROTÁROVÁ, <sup>1</sup>Sebastian GASCON PEREZ, <sup>1</sup>Carolina OLIVER-URRUTIA, <sup>1</sup>Serhii TKACHENKO, <sup>1,2</sup>Karel SLÁMEČKA, <sup>1</sup>Ladislav ČELKO, <sup>1</sup>Edgar B. MONTUFAR

<sup>1</sup>Central European Institute of Technology, Brno University of Technology, Czech Republic,  
[lenka.drotarova@vut.cz](mailto:lenka.drotarova@vut.cz), [eb.montufar@ceitec.vutbr.cz](mailto:eb.montufar@ceitec.vutbr.cz)

<sup>2</sup>Faculty of Mechanical Engineering, Brno University of Technology, Czech Republic, [slamecka@fme.vutbr.cz](mailto:slamecka@fme.vutbr.cz)

<https://doi.org/10.37904/metal.2024.4913>

### Abstract

Additive manufacturing of titanium and its alloys traditionally relies on powder bed fusion techniques, which consume substantial energy. Vat photopolymerization additive manufacturing offers design flexibility similar to powder bed fusion techniques, improved resolution, and a notable reduction in energy consumption. This method involves selectively polymerizing a photosensitive resin by projecting light images of the desired cross-section. While commonly used for polymers and, to a lesser extent, ceramics, its application to produce metallic objects has been restricted due to light scattering hindering resin polymerization. This study initially explores vat photopolymerization and debinding of two commercial resins and their slurries with titanium powder. Secondly, vat photopolymerization was employed to fabricate polymeric porous templates, which were impregnated with a titanium slurry, followed by thermal removal of the template and sintering to consolidate the titanium structure. Faithful replicates of the polymeric template were achieved, demonstrating the potential to create intricate porous titanium structures. To achieve this, optimization of the solid fraction of titanium in the slurry and a refined debinding process are essential to reduce significant shrinkage and prevent chemical contamination during sintering.

**Keywords:** Titanium, vat photopolymerization, replica, sintering

### 1. INTRODUCTION

Additive manufacturing of titanium and its alloys is becoming increasingly important in various advanced industrial sectors, particularly in biomedicine. Currently, the production of titanium and titanium alloys parts predominantly relies on powder bed fusion techniques, especially laser powder bed fusion. These techniques produce heterogeneous metastable microstructures requiring heat treatment post-processing to achieve acceptable properties. Although there are cost-effective alternatives, such as binder jetting [1] and direct ink writing [2], these methods lack the versatility needed for the rapid production of titanium structures with intricate shapes.

Vat photopolymerization (VP) encompasses a range of additive manufacturing techniques known for their low energy consumption, design flexibility similar to powder bed fusion techniques, and high spatial resolution. The spatial resolution of a modern digital light processing printer (DLP) is 10-50  $\mu\text{m}$  on the (X-Y) printing plane and 1  $\mu\text{m}$  the building (Z) direction, while a two-photon polymerization (TPP) printer can achieve resolutions as fine as 150 nm (X-Y) and 10 nm (Z) [3, 4]. VP involves selectively polymerizing a photosensitive resin by projecting light images of the desired cross-section. Various VP approaches utilize different light sources; for instance, DLP utilizes digital mirror device, while TPP uses near-infrared laser.

VP methods are commonly used for processing complex polymeric and ceramic objects. While their application in producing metallic parts has been constrained by high light absorption and scattering, hindering

photosensitive resin polymerization, recent advancements have been made only in VP of copper [5], and nickel alloys [6, 7]. However, the production of titanium structures using VP remains an area of ongoing research. Challenges in VP of titanium arise from the necessity to completely remove the polymerized resin before sintering to ensure high chemical and microstructural quality that meets stringent titanium industrial standards. To initiate this investigation, the study focuses on two methods to fabricate porous titanium structures using the DLP method. Firstly, a titanium slurry for DLP processing was produced using a commercial photosensitive resin, and its photopolymerization and debinding properties were assessed. Secondly, the DLP method was employed to produce porous polymeric templates to be replicated by titanium. The process involves impregnating the VP polymeric templates with a titanium powder, followed by the thermal removal of the template and sintering to consolidate the titanium replica.

## **2. EXPERIMENTAL DETAILS**

### **2.1. Photosensitive resins and titanium powder**

Two commercial low-viscosity resins that polymerizes at 405 nm were utilized in the study: a green basic resin and white a plant-based UV resin (Anycubic Co., Shenzhen, China). The study employed commercially pure argon-atomized titanium spherical powder (ASTM Grade 1; TLS-Technik, Germany) with particles ranging in size from 20 to 63  $\mu\text{m}$ . The use of spherical powder aimed to enhance the fluidity of both powder and slurry.

### **2.2. Slurry preparation and photopolymerization**

The titanium slurry was prepared by blending the photosensitive resin with titanium powder at liquid to powder ratios ranging from 0.12 and 0.33 g/g. The slurry mixing process was conducted in a light-protected environment using a high-shear homogenizer. The fluidity of the slurry was assessed visually by pouring it with a spatula onto a flat surface. The fluidity of the resin alone served as the reference point. Photopolymerization experiments were carried out in a curing station (Wash & Cure 2.0, Anycubic Co., Shenzhen, China) using a power of 25 W at a wavelength of 405 nm. Exposure times ranged from 10 to 600 s.

### **2.3. Thermal elimination of the resin**

The thermal removal of the resin (debinding) was conducted in either air or in a pure argon (purity 4N) atmosphere within the temperature range of 300 to 600  $^{\circ}\text{C}$ . The heating rate was maintained at 1.5  $^{\circ}\text{C}/\text{min}$ , with a consistent dwell time of 12 h in all cases. Ash formation was visually assessed, and the titanium purity was verified by X-ray diffraction (XRD).

### **2.4. Vat photopolymerization of polymeric templates**

Polymeric templates were created using DLP with both basic and plant resins on a bottom-up LCD printing machine (Photon Mono X, Anycubic Co., Shenzhen, China) with a pixel resolution of 50  $\mu\text{m}$  at a wavelength of 405 nm. The 3D models of the templates were designed in computer-aided design software and were saved as stereolithography (STL) files. These STL files were then imported into the printer software. The printing parameters were set as follows: a layer thickness of 50  $\mu\text{m}$ , a standard exposure time of 2 s, an off time of 0.5 s, a bottom exposure time of 28 s, and a bottom layer count of 4. Upon completion of the printing process, any excess unreacted resin on and within the printouts was cleaned with ethanol, followed by an additional curing step at 405 nm for 2 min.

## 2.5. Preparation, debinding, and sintering of replicas

The polymeric templates were submerged in titanium powder, ensuring complete filling of the pore space. Subsequently, any excess powder was gently removed using low-pressure compressed air. The thermal elimination of the polymeric template was performed as outlined in the previous section. Sintering was conducted in a pure argon environment at a temperature of 1400 °C for 10 h. The purity of titanium replicas was assessed by XRD, while the microstructure was examined using an opto-digital light microscope (LM, DSX110, Olympus, Japan) in bright-field (BF) mode and a scanning electron microscope (SEM; Tescan Mira3, Czech Republic) in secondary electron (SE) mode.

## 3. RESULTS AND DISCUSSION

### 3.1. Characterization of titanium slurries

The titanium slurries prepared using the basic resin exhibited suitable fluidity for DLP within the liquid to powder range from 0.33 to 0.25 g/g. In contrast, the slurry prepared with the plant resin demonstrated better fluidity, showing adequacy in the range of 0.33 to 0.14 g/g. Slurries at lower liquid to powder ratios became thick, moldable pastes that were unsuitable for DLP without further additives as they were unable to spread by gravitational flow. To ensure high fluidity and comparable results, a liquid to powder ratio of 0.30 g/g was selected for DLP of both resins.

Photopolymerization experiments in the curing unit revealed that titanium slurries prepared with both basic and plant resins polymerized at 405 nm. However, extended exposure times (5 min for basic resin slurry and 10 min for plant resin slurry) were necessary. Furthermore, the polymerization of the slurry was superficial, with the core of the spread slurry remaining fluid. Lower liquid to powder ratio utilized in further experiments resulted in decreased thickness of the polymerized shell. Therefore, this phenomenon was attributed to the high absorption and reflectivity of metallic titanium at 405 nm, hindering deep penetration of light and activation of the photoinitiator to crosslink the resin.

Despite setting a prolonged exposure time of 1 min, the slurries did not polymerize in the printer. Long exposure times are impractical for DLP as they significantly slow down the printing of sizable objects, reducing competitiveness compared to powder bed fusion additive manufacturing. An alternative was to increase the power, but the printer does not support this option.

Consequently, debinding experiments were performed on resins and slurries polymerized in the curing unit. The basic resin exhibited no decomposition in air at 350 °C (**Figure 1a**). In contrast, at 460 °C the basic resin thermally decomposed generating minimal quantity of ashes (**Figure 1b**). The basic resin was also eliminated from the titanium slurry at 460 °C, but the titanium powder acquired a bluish color (**Figure 1c**). XRD analysis showed that the powder was mainly alpha titanium with some traces of titanium dioxide (rutile, **Figure 1d**).

Similar findings were observed with the plant resin (**Figure 2**). The plant resin did not decompose in air at 350 °C (**Figure 2a**), but decomposition occurred at 410 °C (**Figure 2b**), i.e. 50 °C lower than the basic resin, yielding minimal ash. Unlike the slurry prepared with the basic resin, the titanium powder after debinding acquired a brown color (**Figure 2c**) and the XRD pattern indicated reduced titanium oxidation (**Figure 2d**).

### 3.2. Replica of polymerized resin scaffolds

Quality of encasing the polymeric templates with the titanium powder was high. The powder effectively coated diverse porous structures, including a highly porous cube with a simple cubic unit cell (**Figure 3a**), a spine cage model with an internal gyroid structure (**Figure 3b**), and cylinders with simple cubic, gyroid, diamond, and Schwarz unit cells (**Figure 3c**).

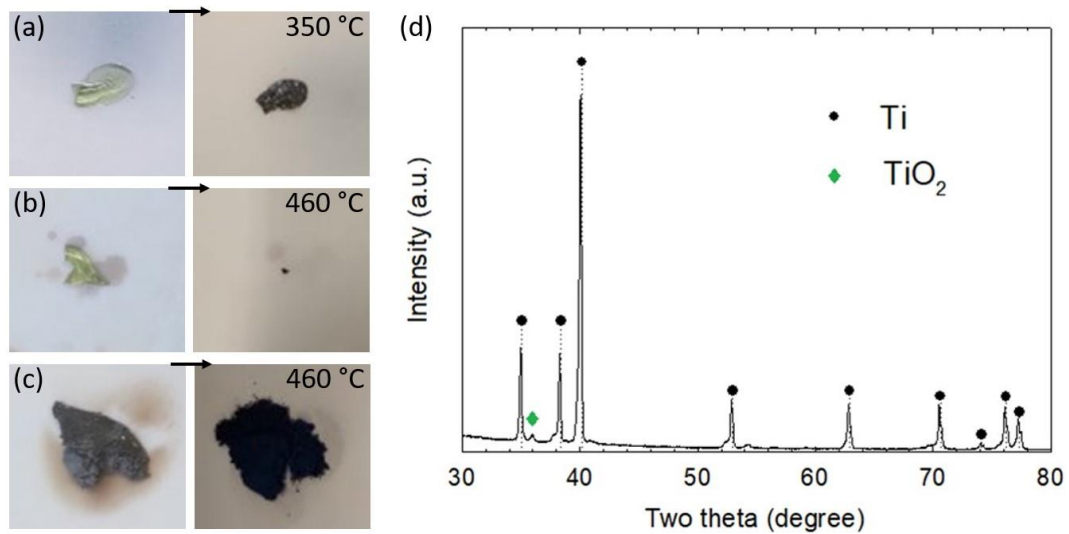


**Figure 1** Debinding a basic resin (a, b) and a resin-powder slurry (c) XRD pattern of debinded slurry (d)

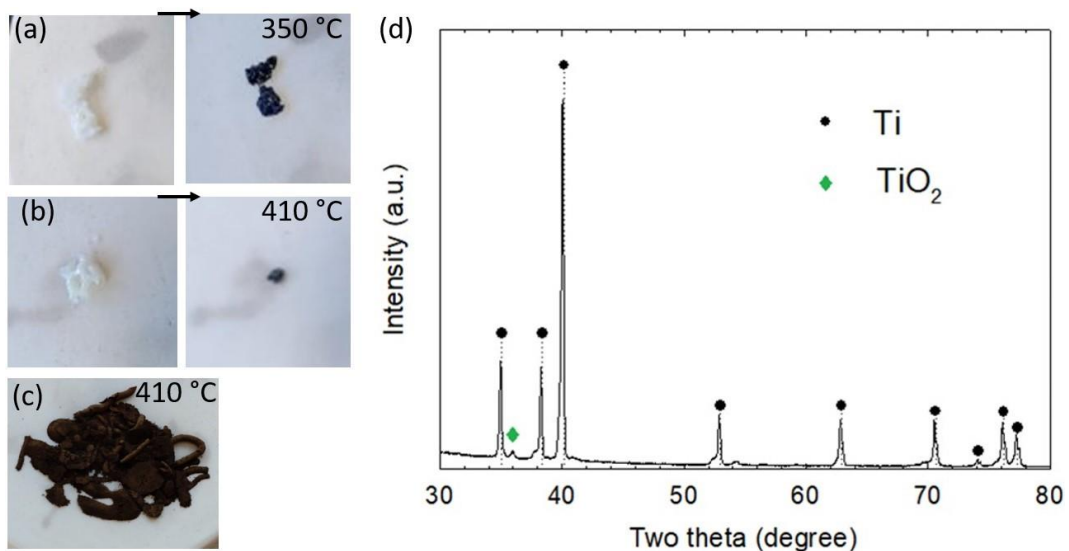


**Figure 2** Debinding a plant resin (a,b) and a of resin-powder slurry (c). XRD pattern of debinded slurry (d)

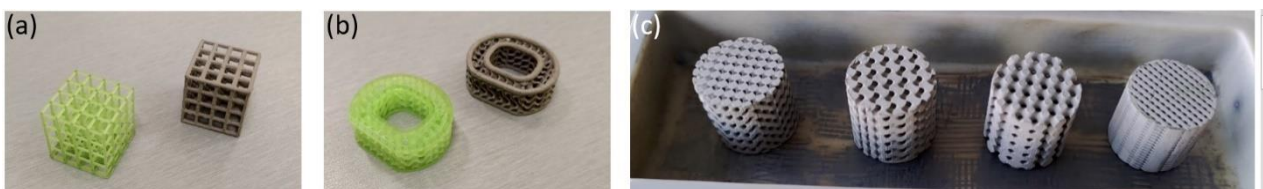


**Figure 3** As-printed and titanium-coated porous polymeric templates in shape of a simple cubic scaffold (a), a spine cage (b). Coated cylindrical templates with simple cubic, gyroid, diamond, and Schwarz unit cells (c)

Upon debinding at 350 °C in air, followed by 600 °C in argon atmosphere, the porous structures exhibited no shrinkage and maintained their geometry (**Figure 4a**). However, the debound structures proved fragile and primarily consisted of titanium carbide according to XRD (**Figure 4b**). Therefore, the carbon residues (ashes) produced at 350 °C in air were not eliminated in argon, leading to their reaction with the titanium powder. Additionally, the XRD pattern displayed a significant hump and contain some XRD reflections attributed to carbon.

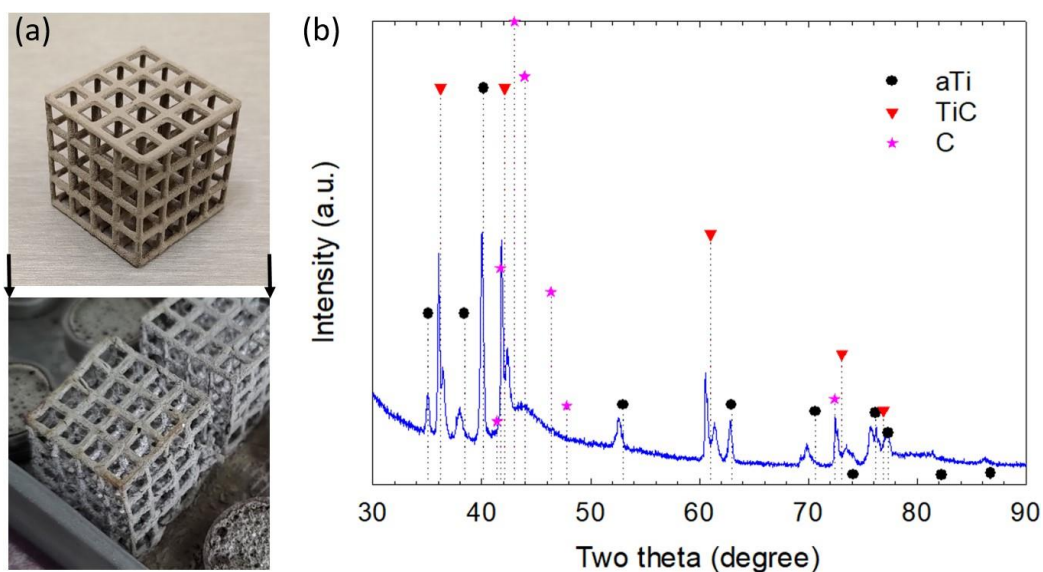


**Figure 4** Replica debinding at 350 °C in air (a) and the XRD pattern of debound structure (b)

The plant-based resin (with lower debinding temperature) was utilized to produce the polymeric templates and was eliminated at 460 °C in an air with the aims of preventing titanium oxidation and totally completely removing carbon to prevent the formation of titanium carbides. The hypothesis was successfully validated by the XRD pattern of the debound powder showed mainly the presence of alpha titanium with minimal rutile content and the absence of carbides or residual carbon signals (**Figure 5c**). However, the polymeric structures experienced a notable shrinkage of nearly 90 % (**Figure 5a**), leading to the detachment of the titanium powder during debinding and the collapse of the structures (**Figure 5b**). In this case, the titanium powder displayed a bluish hue in agreement with the slight oxidation observed by XRD.

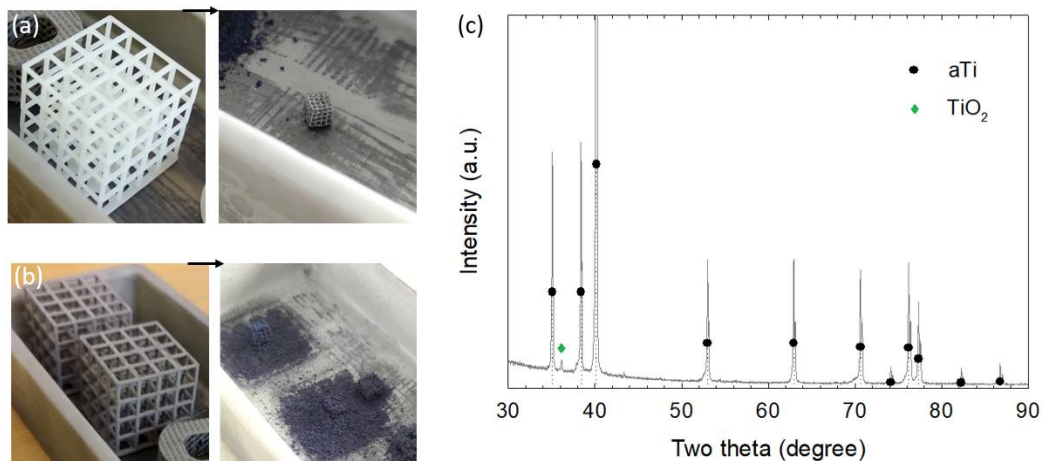


**Figure 5** Template (a) and replica (b) debinding at 460 °C in air. XRD pattern of debound powder (c)

Exploration of debinding in argon at 600 °C followed by sintering at 1400 °C in the same atmosphere revealed moderate shrinkage with the structure retaining its geometry and exhibiting a metallic sheen (**Figure 6a**). The titanium particles developed sintering necks, reaching the intermediate state of sintering where spherical particles were remained distinguishable, and significant interparticle porosity was evident. The resulting sintered structures were sufficiently strong and stable, without releasing loose powder. XRD analysis (**Figure 6b**) indicated that the sintered scaffolds comprised a blend of titanium carbide, metallic titanium, and carbon, with minimal oxide content. The present results show that the challenge in producing pure titanium porous

structures by replica of VP templates lies in finding a balance between structural shrinkage due to resin removal and ensuring complete elimination to prevent carbide formation.

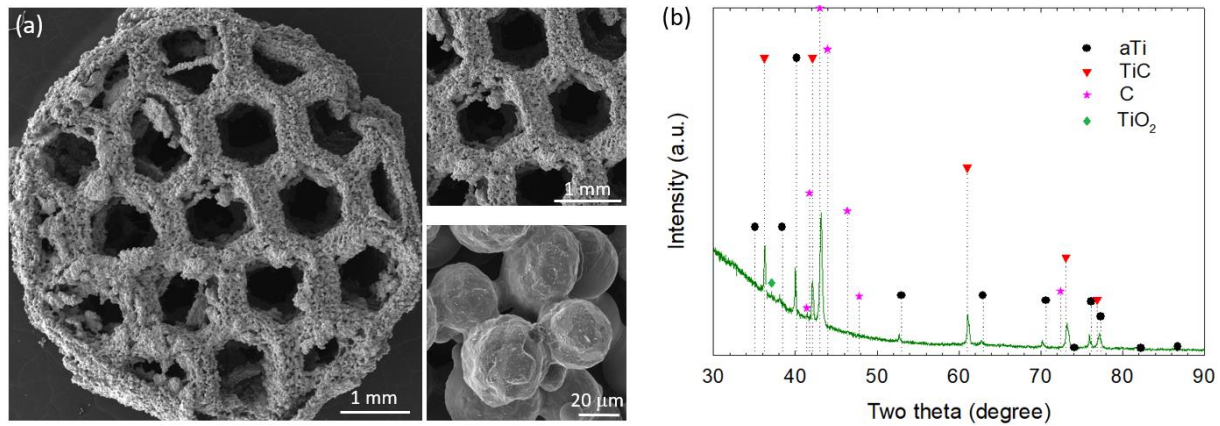


**Figure 6** The structural overview of the sintered replica (a) and its XRD pattern (b)

#### 4. CONCLUSION

This study represents the initial attempt to fabricate titanium structures using vat photopolymerization. Almost complete thermal elimination of used resins in air was attained at the temperatures of 460 °C (basic resin) and 410 °C (plant resin). The photopolymerization process of titanium slurries was hindered by limited light penetration depth, which required extended exposure time. Debinding investigations of photopolymerized slurries revealed the presence of alpha titanium with minor rutile traces. Subsequently, VP polymeric templates of diverse shapes were coated with titanium. The debinding and sintering of templates highlighted the need for optimization of both steps to fully eliminate the resin and avoid structural contamination by carbon.

#### ACKNOWLEDGEMENTS

*This work was supported by the Czech Science Foundation under project number 23-07879S.*

#### REFERENCES

- [1] LI, M., DU, W., ELWANI, A., PEI, Z., MA, C. Metal binder jetting additive manufacturing: A literature review. *Journal of Manufacturing Science and Engineering*. 2020, vol. 142, pp. 090801.
- [2] OLIVER-URRUTIA, C., KASHIMBETOVA, A., SLÁMEČKA, K., ČELKO, L., MONTUFAR, E.B. Robocasting additive manufacturing of titanium and titanium alloys: A review. *Transactions of the Indian Institute of Metals*. 2022, vol. 76, pp. 389-402.
- [3] ZHANG, F., ZHU, L., LI, Z., WANG, S., SHI, J., TANG, W., LI, N., YANG, J. The recent development of vat photopolymerization: A review. *Additive Manufacturing*. 2021, vol. 48, pp. 102423.
- [4] DELEEP, C., JACOB, L., SHEBEEB, M.C., UMER, R., BUTT, H. Review of vat photopolymerization 3D printing of photonic devices. *Additive Manufacturing*. 2024, In Press, pp. 104189.
- [5] JAVED, A., SHAH, O.R., AHMAD, S., AHMED, D. Optimization of viscosity and composition of mixture of Cu powder and acrylate based resin for vat photopolymerization of metal components. *Results in Engineering*. 2023, vol. 19, pp. 101307.
- [6] MOUSAPOUR, M., PARTANEN, J., SALMI, M. NiTiCu alloy from elemental and alloyed powders using vat photopolymerization additive manufacturing. *Additive Manufacturing*. 2023, vol. 78, pp. 103853.
- [7] ZHANG, Y., LI, S., LIU, X., LI, X., DUAN, W., LI, L., LIU, B. JAVED, A., SHAH, O.R., AHMAD, S., AHMED, D. Additive manufacturing and characterization of microstructure evolution of Inconel 718 superalloy produced by vat photopolymerization. *Additive Manufacturing*. 2023, vol. 61, pp. 103367.